Hindawi Publishing Corporation
Dataset Papers in Physics
Volume 2013, Article ID 926470, 5 pages
http://dx.doi.org/10.1155/2013/926470

Dataset Paper

Optical Constants of α- and β-Zinc(II)-Phthalocyanine Films

Michael Kozlik, Sören Paulke, Marco Gruenewald, Roman Forker, and Torsten Fritz

Institute of Solid State Physics, Friedrich Schiller University Jena, Helmholtzweg 5, 07743 Jena, Germany

Correspondence should be addressed to Torsten Fritz; torsten.fritz@uni-jena.de

Received 16 November 2012; Accepted 17 December 2012

Academic Editors: T.-H. Fang, S. Kiravittaya, S. K. Kulshreshtha, and H.-P. Wagner

We present a dataset of the optical constants of α- and β-zinc(II)-phthalocyanine (ZnPc). They were determined accurately from transmission and differential reflectance spectra, with the surface roughness taken into account. For this purpose, thin films were prepared on quartz glass substrates via physical vapor deposition and characterized by ultraviolet-visible (UV-Vis) spectroscopy before as well as after a well-defined annealing process. Kramers-Kronig consistency of the optical constants obtained was checked by means of a numerical algorithm.

1. Introduction

Zinc(II)-phthalocyanine (ZnPc) is a promising material for organic electronics, especially photovoltaic devices. It has already been applied in prototypes of solar cells [1–4]. Furthermore, it is already known that phthalocyanines (including ZnPc) can exist in multiple types of crystalline phases [5]; in particular, the metastable α-ZnPc (higher electrical conductivity) and the stable β-ZnPc (lower electrical conductivity) [6] need to be distinguished. Structural analysis of both phases and detailed information about the phase transition as shown in [7] are needed to set suitable constraints for a numerical model to determine the optical constants of α- and β-ZnPc. Once the optical constants are known, they can be used for modeling layer systems or even photovoltaic devices, or vice versa, for a nondestructive optical analysis of the crystallinity of ZnPc layers. Here, we present a reliable method for the determination of optical constants of organic thin films, where the surface roughness is taken into account. Finally, we present a detailed dataset of optical constants for polycrystalline α- and β-ZnPc covering an energy interval from 1.2 eV to 5.0 eV.

2. Methodology

Thin films of ZnPc were prepared via physical vapor deposition on quartz glass. Quartz glass was used as substrate due to the low absorbance in a broad spectral range ($k < 10^{-7}$ between 300 nm and 850 nm). After thorough in situ degassing, the ZnPc powder obtained from Sigma-Aldrich with 97% chemical purity was thermally evaporated from a ceramic crucible in a tungsten boat and deposited at a rate of 0.6 Å/s under high vacuum conditions (pressure: $p \sim 10^{-5}$ mbar). To realize the growth of the α phase, ZnPc was deposited on substrates kept at room temperature [8]. A phase transition from α-ZnPc to β-ZnPc upon annealing has been demonstrated in the literature [7, 9, 10]. Here, the stable β-ZnPc phase was obtained from the metastable α-ZnPc samples via annealing under ambient conditions for 3 h at 240°C and above. Films of both phases with different thicknesses from 30 nm up to 150 nm were examined by means of a Varian Cary 5000 UV-Vis spectrophotometer. The transmission measurements were done using a light beam perpendicular to the sample surface, while the angle of incidence is 12° in reflection geometry. In both cases, unpolarized light was used. The spectrophotometer was operated in a dual-channel mode which enhances the long-term (several hours) stability significantly. The scanning velocity was set to 300 nm/min (averaging time: 0.2 s) in the NIR region and 120 nm/min (averaging time: 0.5 s) in the UV-Vis region with a fixed spectral bandwidth of 5 nm and 4 nm, respectively. The resulting resolution is by far sufficient for the typical linewidths of organic thin films at room temperature. The measured optical spectra were analyzed by a numerical algorithm implemented in Wolfram Mathematica 8 in order to extract the complex refractive index $\hat{n}(E) = n(E) - ik(E)$

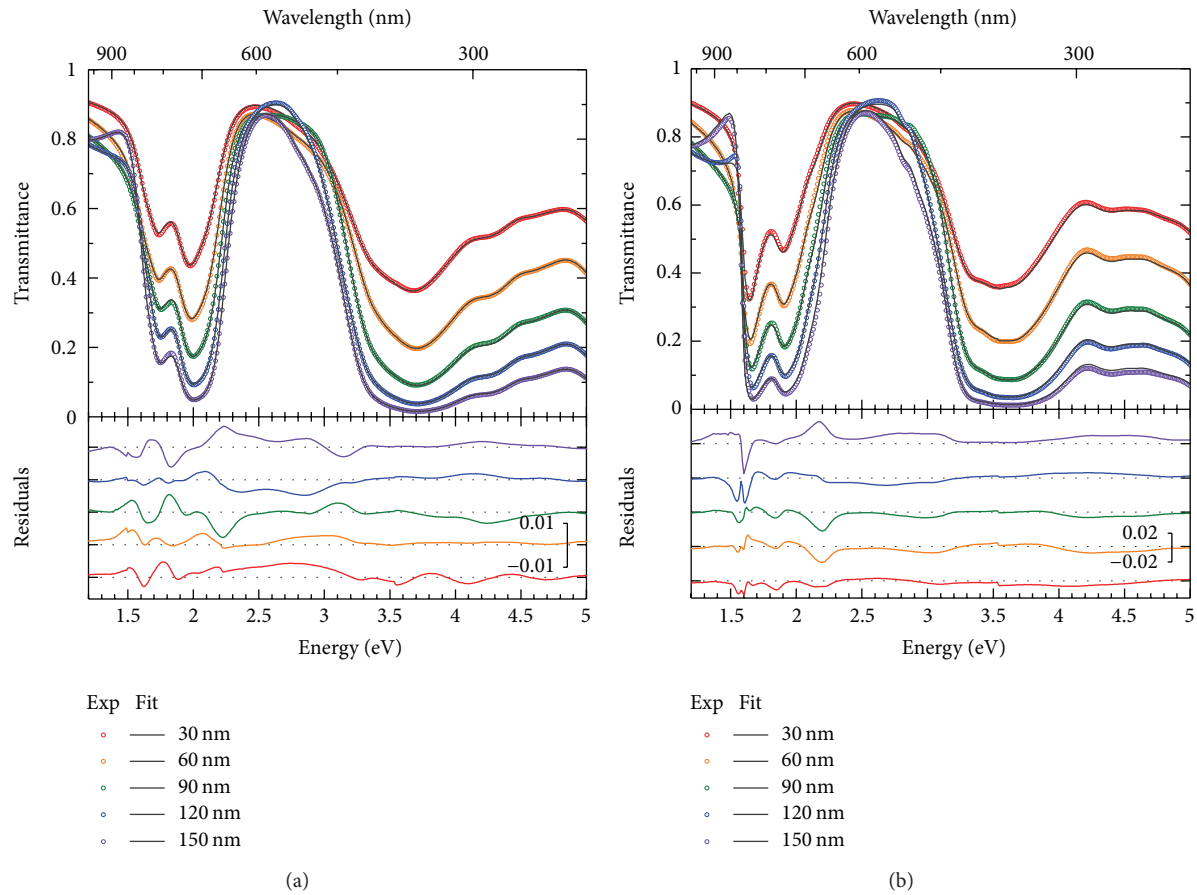

FIGURE 1: Experimental dataset (open symbols) consisting of (a) 5 samples of α-ZnPc and (b) 5 samples of β-ZnPc with various nominal thicknesses, characterized by one transmittance curve each, and the curves which were fitted with a single set of optical constants used for all layer thicknesses (solid line). In the lower part, the residuals $T_{th} - T_{exp}$ of the fitting process are shown. For the sake of clarity, subsequent residual spectra are displayed with a vertical offset. The insets show the respective scale bars for the residuals. The nominal film thicknesses are given.

of the thin film, where $n(E)$ and $k(E)$ denote the photon-energy-dependent refractive index and extinction coefficient, respectively.

The determination of the optical constants is possible by means of a simultaneous analysis of transmission (T) and reflectance (R) spectra. However, here the reflectance data were replaced by differential reflectance spectra (DRS) [11–13]. Thereby, the need for a calibrated mirror can be avoided. In the following, the basic ideas of the numerical algorithm will be explained. In order to interpret the measured optical spectra of ZnPc thin films, the numerical treatment is based on a layer model, consisting of the substrate and the organic thin film as well. We used the generalized matrix formalism based on the Fresnel formulas for mixed coherent and incoherent layers as outlined in [14]. In order to improve our layer model, we analyzed the interfaces by non-contact atomic force microscopy (nc-AFM) [7]. Accordingly, the root-mean-square (rms) roughness (sometimes also denoted by the symbol R_q) of as-deposited as well as annealed films of ZnPc was found to be small but not insignificant with respect to the film thickness d (rms/d < 20% for α-ZnPc and rms/d < 5% for β-ZnPc). Hence, for an accurate determination of the optical constants, the values obtained for the surface roughness at the air-to-ZnPc interface have to be taken into account. This was done by modified Fresnel coefficients considering only partial coherence due to phase differences of the transmitted and reflected beams by Gaussian-distributed irregularities as outlined in [15]. Because of the azimuthal orientation of the grains, the in-plane component of the optical anisotropy can be neglected. The substrate was treated as incoherent due to its rather large thickness (0.63 mm) with respect to the coherence length of the light. This means that we indeed account for multiple reflections at both substrate interfaces but internal interference effects do not contribute to the signal. An optical characterization of the quartz glass substrate used was done by transmission measurements in the UV, visual, and near-infrared spectral region in order to extract the refractive index individually assuming negligible absorption ($k = 0$).

As a matter of fact, no dispersion model for ZnPc is required in the calculation. Accordingly, the algorithm starts with a set of optical constants, that is, the refractive index $n(E_1, \ldots, E_i, \ldots, E_N)$ and the extinction coefficient $k(E_1, \ldots, E_i, \ldots, E_N)$, each consisting of N points to be fitted to

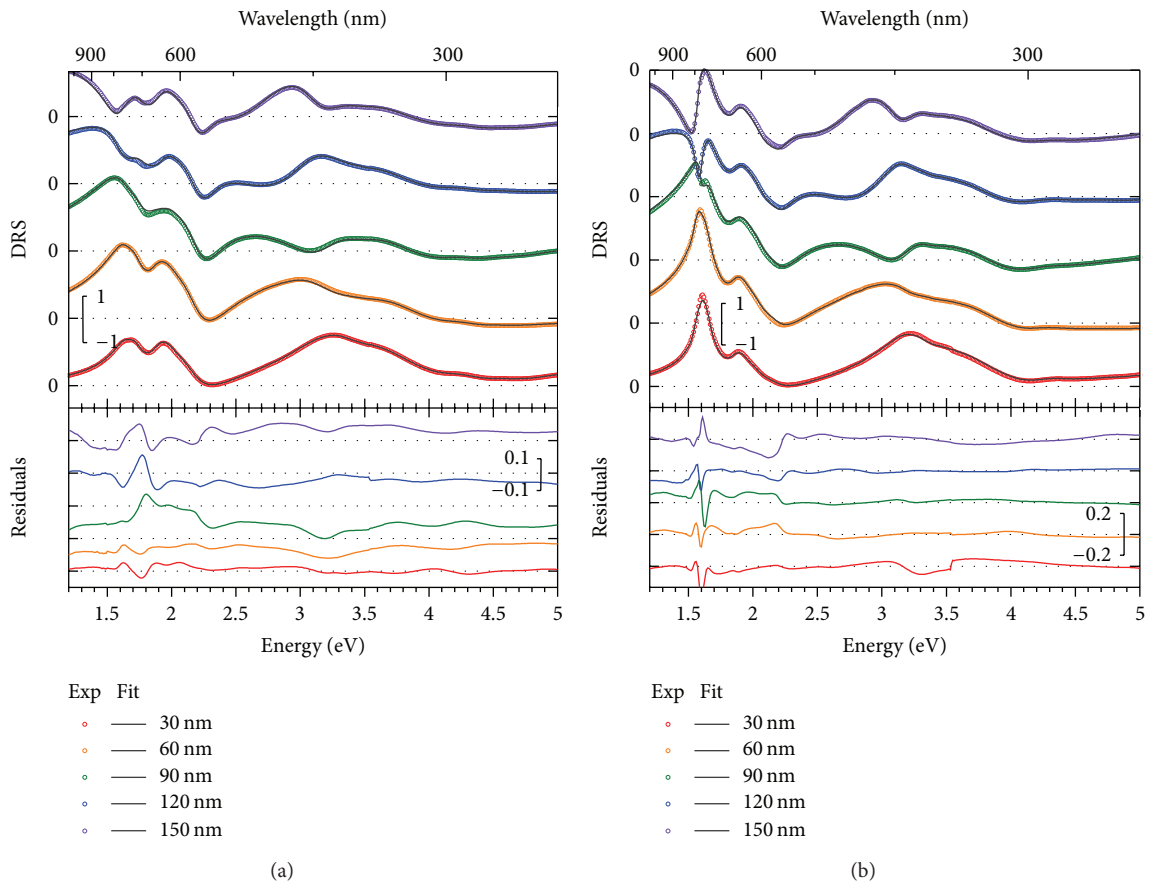

FIGURE 2: DRS signal (open symbols) of (a) α-ZnPc and (b) β-ZnPc and the fitted curves (solid lines). In the lower part, the residuals of the fitting process are shown. For the sake of clarity, the spectra are displayed with a vertical offset. The insets show the respective scale bars.

the experimental data. In this work, the energy interval from 1.2 eV to 5.0 eV with a step size of 0.01 eV results in an N of 381. If only one pair of transmission and differential reflectance spectra is used for the extraction of the optical constants n and k, then the film thickness needs to be specified precisely to prevent the algorithm to produce large errors in the optical constants or even to get stuck in a nonphysical solution. Several optical spectra which are not necessarily of the same optical quantity analyzed in parallel using the same values for the refractive index $n(E)$ and the extinction coefficient $k(E)$ of the thin film for all spectra were used to overcome this issue, as suggested in [16]. Consequently, five samples with nominal thicknesses of 30 nm, 60 nm, 90 nm, 120 nm, and 150 nm, respectively, were measured (nominal thicknesses being determined with a quartz crystal microbalance). The objective function to be minimized is

$$\delta = \sum_{j}\sum_{i=1}^{N} A^{(j)}(E_i) \times \left\{X_{\text{th}}^{(j)}\left(n(E_i), k(E_i)\right) - X_{\text{exp}}^{(j)}(E_i)\right\}^2 \xrightarrow{n,k \text{ variation}} \min, \quad (1)$$

where $X_{\text{th}}^{(j)}$ denotes any calculated quantity (e.g., transmission or DRS) to be fitted to the respective experimental data $X_{\text{exp}}^{(j)}$. The index j is used to distinguish between the different samples with different thicknesses. Each signal of T and DRS was weighted by a factor $A^{(j)}(E)$ as described in [17] in order to equalize the information $X^{(j)}(E)$ from all spectra having originally different magnitudes. $A^{(j)}(E)$ is calculated from the minimal ($n = 1, k = 0$) and maximal ($n = 3, k = 1$) values of the refractive index and extinction coefficient expected for phthalocyanine thin films [16]. The advantage of this procedure is that the layer thickness can be optimized as well using the nominal thicknesses as starting values. By doing so, it is important to cover an appropriate thickness range of layers fitted simultaneously as only thickness-dependent internal interference effects contribute significant new information to the fitting procedure. Moreover, it was found that the fit is then rather robust against different starting values for the film thickness even if they are far from real. The rms values were treated as fitting parameters likewise, except the first rms value which belongs to the 30 nm ZnPc film where no significant gradient in the objective function was found. The fit itself was carried out by means of a Levenberg-Marquardt algorithm.

Figures 1 and 2 show the fitted spectra for both phases of ZnPc as well as the corresponding residuals of the fit for the transmittance and the DRS signals, respectively. In Figure 3,

Table 1: Nominal and optimized values of film thickness and rms values of the samples used for the determination of optical constants. The errors given are statistical errors from the fitting procedure.

Nominal thickness (nm)	α-ZnPc		β-ZnPc	
	Optimized thickness (nm)	rms (nm)	Optimized thickness (nm)	rms (nm)
30	36.95 ± 0.03	1.1 ± 0.3	36.15 ± 0.05	—
60	65.30 ± 0.04	3.1 ± 0.2	61.90 ± 0.07	5.4 ± 0.2
90	96.63 ± 0.04	7.7 ± 0.1	94.65 ± 0.08	4.5 ± 0.1
120	132.15 ± 0.05	10.6 ± 0.1	129.09 ± 0.07	5.9 ± 0.1
150	168.90 ± 0.07	13.2 ± 0.1	167.88 ± 0.07	5.6 ± 0.1

the resulting spectra of the optical constants for α-ZnPc and β-ZnPc are shown. Furthermore, the optimized film thicknesses and respective rms values including the standard deviations of the fit are shown in Table 1.

The optical constants for α-ZnPc and β-ZnPc thin films obtained reproduce the spectral measurements very nicely. As one can see, the residuals are very small compared to the transmission data. The edge at 350 nm (3.54 eV) is caused by the internal light source changeover of the spectrophotometer used but is smaller than the mean residuals and therefore has no significant influence.

The results were checked afterwards for Kramers-Kronig consistency. As described by Nitsche et al. [17], the integral can be split into an additive offset which is energy independent and an integral the over important region (1.2 eV to 2.6 eV: energetically lowest optical absorption band) which shows the spectral characteristics to be analyzed. In this region, model-free Kramers-Kronig consistency was confirmed. The numerically obtained rms values are in very good agreement with those from our own nc-AFM images [7] and those presented in [18]. Without considering the surface roughness, the fit is less suitable which results in slightly different optical constants, especially in the ultraviolet spectral region. Our data of α-ZnPc compare favorably with those of the almost identical molecule copper(II)-phthalocyanine (CuPc, α-phase) from [16, 19].

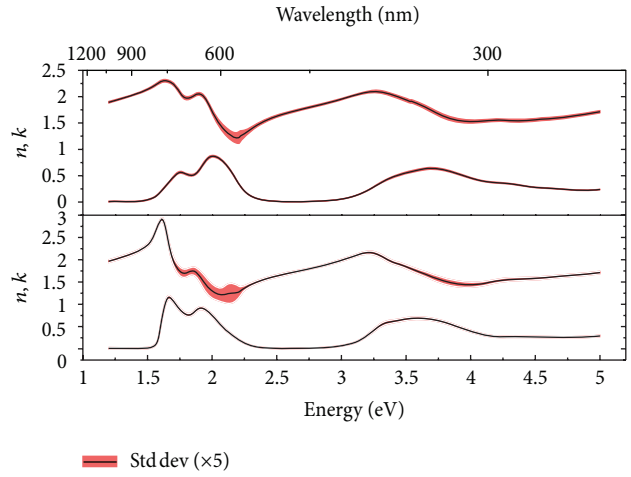

Figure 3: Spectra of refractive index n and extinction coefficient k of α- (top) and β- (bottom) ZnPc, respectively. The standard deviation (statistical errors from the fitting procedure, enlarged 5 times) is indicated by the reddish error margin.

3. Dataset Description

The dataset associated with this Dataset Paper consists of 5 items which are described as follows.

Dataset Item 1 (Spectra). Spectra of 5 samples of α-ZnPc with various nominal thicknesses, characterized by one transmittance curve each (open symbols), and the curves which were fitted with a single set of optical constants used for all layer thicknesses (solid line). In the lower part, the residuals $T_{th} - T_{exp}$ of the fitting process are shown. For the sake of clarity, subsequent residual spectra are displayed with a vertical offset.

Dataset Item 2 (Spectra). Spectra of 5 samples of β-ZnPc with various nominal thicknesses, characterized by one transmittance curve each (open symbols), and the curves which were fitted with a single set of optical constants used for all layer thicknesses (solid line). In the lower part, the residuals $T_{th} - T_{exp}$ of the fitting process are shown. For the sake of clarity, subsequent residual spectra are displayed with a vertical offset.

Dataset Item 3 (Spectra). DRS signal (open symbols) of α-ZnPc and the fitted curves (solid lines). In the lower part, the residuals of the fitting process are shown. For the sake of clarity, the spectra are displayed with a vertical offset.

Dataset Item 4 (Spectra). DRS signal (open symbols) of β-ZnPc and the fitted curves (solid lines). In the lower part, the residuals of the fitting process are shown. For the sake of clarity, the spectra are displayed with a vertical offset.

Dataset Item 5 (Spectra). Spectra of refractive index n and extinction coefficient k of α- (top) and β- (bottom) ZnPc, respectively. The standard deviation (statistical errors from the fitting procedure, enlarged 5 times) is indicated by the reddish error margin.

4. Concluding Remarks

Different crystalline phases of ZnPc, namely, α-ZnPc and β-ZnPc, have been characterized optically via UV-Vis spectroscopy. Reliable data for the optical constants of both zinc(II)-phthalocyanine phases could be determined when the surface roughness was taken into account. Kramers-Kronig consistency was confirmed numerically afterwards.

Dataset Availability

The dataset associated with this Dataset Paper is dedicated to the public domain using the CC0 waiver and is available at http://dx.doi.org/10.1155/2013/926470/dataset.

Disclosure

The authors do not have a direct financial relation with the commercial identities mentioned in the paper that might lead to conflict of interests for any of the authors.

Acknowledgments

The financial support by the Thüringer Ministerium für Bildung, Wissenschaft und Kultur Grant no. B515-10030 and by the Deutsche Forschungsgemeinschaft (DFG) Grant nos. FR875/9 and FR875/11 is gratefully acknowledged. The authors thank Prof Dr. Carsten Ronning for making his equipment for optical spectroscopy available to them.

References

[1] I. Kim, H. M. Haverinen, Z. Wang et al., "Efficient organic solar cells based on planar metallophthalocyanines," *Chemistry of Materials*, vol. 21, pp. 4256–4260, 2009.

[2] C. Florica, I. Arghir, and L. Ion, "Production and characterization of CdTe wire arrays for hybrid inorganic/organic photovoltaic cells," *Digest Journal of Nanomaterials and Biostructures*, vol. 6, no. 1, pp. 21–27, 2011.

[3] L.-C. Chen and B.-H. Liu, "Porous silicon layer patterned from anodic aluminum oxide and application in ZnPc hybrid solar cell," *Electrochemical and Solid-State Letters*, vol. 13, no. 4, pp. H108–H111, 2010.

[4] S. Bereznev, R. Koeppe, I. Konovalov et al., "Hybrid solar cells based on $CuInS_2$ and organic buffer-sensitizer layers," *Thin Solid Films*, vol. 515, no. 15, pp. 5759–5762, 2007.

[5] A. A. Ebert and H. B. Gottlieb, "Infrared spectra of organic compounds exhibiting polymorphism," *Journal of the American Chemical Society*, vol. 74, no. 11, pp. 2806–2810, 1952.

[6] K. Wihksne and A. E. Newkirk, "Electrical conductivities of α- and β-phthalocyanine," *Journal of Chemical Physics*, vol. 34, pp. 2184–2185, 1961.

[7] M. Kozlik, S. Paulke, M. Gruenewald, R. Forker, and T. Fritz, "Determination of the optical constants of α- and β-zinc (II)-phthalocyanine films," *Organic Electronics*, vol. 13, no. 12, pp. 3291–3295, 2012.

[8] F. W. Karasek and J. C. Decius, "Observations concerning polymorphic crystalline modifications of the phthalocyanines," *Journal of the American Chemical Society*, vol. 74, no. 18, pp. 4716–4717, 1952.

[9] S. Kment, P. Kluson, M. Drobek et al., "Preparation of thin phthalocyanine layers and their structural and absorption properties," *Thin Solid Films*, vol. 517, no. 17, pp. 5274–5279, 2009.

[10] L. Gaffo, M. R. Cordeiro, A. R. Freitas, W. C. Moreira, E. M. Girotto, and V. Zucolotto, "The effects of temperature on the molecular orientation of zinc phthalocyanine films," *Journal of Materials Science*, vol. 45, no. 5, pp. 1366–1370, 2010.

[11] H. Proehl, R. Nitsche, T. Dienel, K. Leo, and T. Fritz, "*In situ* differential reflectance spectroscopy of thin crystalline films of PTCDA on different substrates," *Physical Review B*, vol. 71, no. 16, Article ID 165207, 14 pages, 2005.

[12] R. Forker and T. Fritz, "Optical differential reflectance spectroscopy of ultrathin epitaxial organic films," *Physical Chemistry Chemical Physics*, vol. 11, no. 13, pp. 2142–2155, 2009.

[13] R. Forker, M. Gruenewald, and T. Fritz, "Optical differential reflectance spectroscopy on thin molecular films," *Annual Reports on the Progress of Chemistry C*, vol. 108, pp. 34–68, 2012.

[14] E. Centurioni, "Generalized matrix method for calculation of internal light energy flux in mixed coherent and incoherent multilayers," *Applied Optics*, vol. 44, no. 35, pp. 7532–7539, 2005.

[15] C. C. Katsidis and D. I. Siapkas, "General transfer-matrix method for optical multilayer systems with coherent, partially coherent, and incoherent interference," *Applied Optics*, vol. 41, no. 19, pp. 3978–3987, 2002.

[16] T. Fritz, J. Hahn, and H. Böttcher, "Determination of the optical constants of evaporated dye layers," *Thin Solid Films*, vol. 170, no. 2, pp. 249–257, 1989.

[17] R. Nitsche and T. Fritz, "Precise determination of the complex optical constant of mica," *Applied Optics*, vol. 43, no. 16, pp. 3263–3270, 2004.

[18] C. Schünemann, C. Elschner, A. A. Levin, M. Levichkova, K. Leo, and M. Riede, "Zinc phthalocyanine—influence of substrate temperature, film thickness, and kind of substrate on the morphology," *Thin Solid Films*, vol. 519, no. 11, pp. 3939–3945, 2011.

[19] A. B. Djurišić, C. Y. Kwong, T. W. Lau et al., "Optical properties of copper phthalocyanine," *Optics Communications*, vol. 205, no. 1–3, pp. 155–162, 2002.